Geophys. J. R. astr. Soc. (1987) **91**, 287–311

Shear-wave polarizations near the North Anatolian Fault - III. Observations of temporal changes.

Tian-Chang Chen *Seismological Bureau of Sichuan Province, Chendu, Sichuan, China*

David C. Booth and Stuart Crampin *British Geological Survey, Murchison House, West Mains Road, Edinburgh EH9 3LA, Scotland UK*

Accepted 1987 July 28. Received 1987 July 27; in original form 1987 March 12

Summary. Almost all shear-waves from local earthquakes recorded on closely-spaced three-component seismometer networks deployed near the North Anatolian Fault, Turkey, in two experiments in 1979 and 1980, display shear-wave splitting. The observations are consistent with the presence of EDA (extensive-dilatancy anisotropy), distributions of fluid-filled cracks and microcracks aligned by the regional stress field. Temporal changes in the stress-field, which may occur before an earthquake, may modify the geometry and possibly the orientation of the EDA-microcracks, and lead to corresponding changes in the behaviour of the split shear-waves. A third experiment was undertaken in 1984 to investigate EDA further and to search for possible temporal variations of the polarization of the leading split shear-wave and the time delay between split shear-waves. Observations indicate that the polarization alignments, which are parallel to the strike of the parallel vertical EDA-cracks, are unaltered between 1979 and 1984, implying that the direction of the regional stress field has not changed significantly. Temporal changes in the stress field are more likely to cause changes in the crack density and/or aspect ratio, which would result in a corresponding change in time delay between the split shear-waves. We examine observations of time delay in relation to their propagation path with respect to the crack geometry since it is then possible to separate the effects of changes in crack density and changes in aspect ratio. With this procedure, a small temporal variation of time delays is found between 1979 and 1984, consistent with a decrease in crack density, and consequently a relaxation of stress, in this time period. No evidence was found for any observable variation of time delay over a six month observation span in 1984. We suggest that analysis of repeated shear-wave VSPs offers a technique for monitoring stress changes before earthquakes.

1 Introduction

Shear waves propagating through effectively anisotropic media, such as aligned crystals or aligned cracks, split into two or more arrivals with different velocities and different polarizations. The split arrivals insert characteristic signatures into the shear wavetrain, even in weakly anisotropic media. Since all stress-induced cracks are likely to be aligned and hence effectively anisotropic, Crampin (1978) suggested that it might be possible to monitor dilatancy through observations of shear-wave splitting. To test this suggestion, Turkish Dilatancy Projects TDP1 (in 1979) and TDP2 (in 1980) were set up to record three-component shear-waves from a swarm of small earthquakes near the North Anatolian Fault in Turkey (Crampin *et al.* 1980; 1985). Booth *et al.* (1985) and Crampin & Booth (1985) showed that the shear-wave data exhibited splitting and polarization alignments consistent with an interpretation in terms of crack-induced anisotropy aligned by the local stress field.

Shear-wave splitting due to stress-aligned crack-anisotropy has since been identified in a large number of records of shear-waves recorded in a variety of tectonic regimes; these observations have been summarized in Crampin (1987a). The presence of similar alignments of shear-wave polarizations over a wide region surrounding small earthquakes, together with industrial shear-wave reflection profiles and VSP experiments (Crampin 1987b), indicate that the stress-aligned cracks can exist almost everywhere in the crust.

An explanation for the presence of aligned cracks in a region of low ambient deviatoric stress is given by the hypothesis of extensive-dilatancy anisotropy or EDA (Crampin *et al.* 1984). Crampin *et al.* (1984) suggest that the fluid-filled cracks and pores which are likely to exist in most crustal rocks (Crampin & Atkinson 1985) are aligned by stress in processes such as subcritical crack growth (Atkinson 1984) so that the cracked rock becomes effectively anisotropic to seismic wave propagation (Crampin 1978). The EDA hypothesis offers a technique for *in situ* monitoring of changes in stress within the rockmass. For instance, a change in the direction or magnitude of the local stress-field may modify the geometry of the crack distribution ution in the rock mass, causing changes in the behaviour of the split shear-waves. Thus analysis of shear-wave splitting should allow changes in crack configuration, and hence changes in stress, to be monitored. This offers a potential technique for following the earthquake stress cycle, and possibly prediction, through the detection and monitoring of temporal changes in split shear-wave characteristics.

The two characteristics which it is possible to measure and analyse in records from local earthquakes are (1) the polarization direction of the first shear-wave, and (2) the time delay between the split shear-waves. Peacock *et al.* (1987) examined records of small local earthquakes near the Anza seismic gap on the San Jacinto fault in Southern California, covering a period of two years. They observed shear-wave splitting, the characteristics of which were consistent with the presence of EDA-cracks. There was no evidence of any temporal change in polarization direction, but a statistically significant increase with time of the delays between the split shear waves was observed at one station. They attributed the change to elastic "bowing" (increase in aspect ratio) of microcracks due to increased tension normal to the crack face, or increased compression parallel to the crack face, as the stress changes before an impending earthquake.

In 1984, a third TDP network (TDP3) was deployed, and recorded local events over a period of six months near the North Anatolian fault, in the same area as TDP1 and TDP2. One of the objectives of this experiment was to determine if the shear-wave characteristics observed during TDP1 and TDP2 showed any form of temporal variation in the intervening four years. In this paper we examine the TDP data recorded in 1979, 1980, and 1984 for evidence of temporal changes in the shear wave splitting.

2 The TDP3 seismic network

The closely-spaced network of nine three-component seismic stations deployed during the TDP3 experiment, May-November 1984, is shown in Fig. 1. Stations TE, SE, AY, ME, and PA were also occupied during TDP1, and stations TE, SE, AY, DP, and PB during TDP2. Stations PA and KD were occupied for only limited periods of time during TDP3, and KS was not fully operational over the whole period. The stations recorded local earthquake swarm activity beneath and to the south of the southern limit of the graben structure which defines the North Anatolian Fault in this region (Evans *et al.* 1985). The swarm events are located at depths of 6-15 km within an area approximately 15 km in diameter. A map of the best-located earthquake epicentres for the period of the TDP3 experiment is shown in Lovell *et al.* (1987). As in the case of the TDP1 and TDP2 data, almost all of the several hundred shear wavetrains recorded within the shear-wave window (Booth and Crampin 1985) show the abrupt changes in polarization which are characteristic of shear-wave splitting. Examples of shear-wave splitting in seismograms recorded during TDP3 are shown in the Appendix.

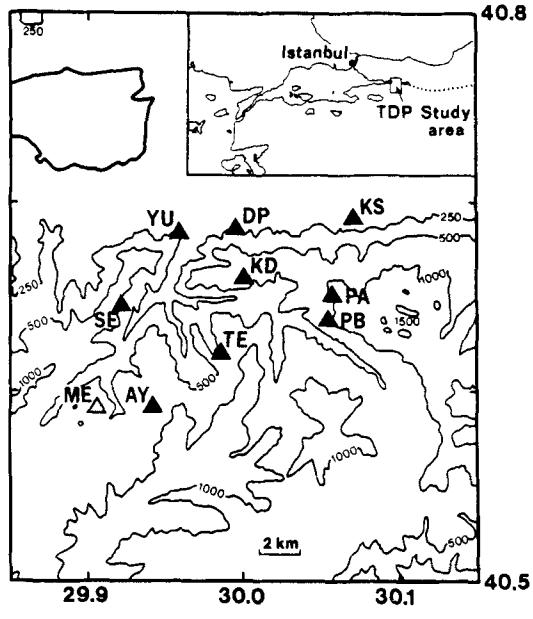

Figure 1. Location of the three-component TDP3 stations deployed in 1984 (solid triangles), and station ME (open triangle) deployed only in 1979. Contour lines represent heights in metres. The inset map of Northwestern Turkey shows the position of the study area and the surface break of the North Anatolian Fault (dotted line).

3 Parameterization of shear-wave splitting

In ideal circumstances, four parameters can be used to characterize the shear-wave splitting observed at a recorder. These are the polarization direction of (1) the first and (2) the second split shear-waves arrivals, (3) the time delay between the split shear-waves; and (4) their relative attenuation. Unfortunately, only two of these, (1) and (3), are available for monitoring shear-waves from earthquake sources recorded at the surface. The most reliable observation is the polarization of the first split shear-wave, as the polarization is controlled by the direction of propagation through the anisotropic symmetry. Since the alignment is caused by the regional stress-field, it is likely to be the same over a considerable volume. The arrival of the second split shear-wave is characterised by an abrupt change in direction or ellipticity in the particle motion of the first split shear-wave. The precise onset of this change is often difficult to identify for reasons given in the Appendix, where we describe a procedure which reduces the subjective nature of the measurement of time delays between split shear-waves. The polarization of the second split shear-wave is rarely clearly visible, since it is

superimposed on the first shear-wave, as well as the background noise and the P-wave coda. Measurement of the relative attenuation between the two shear-wave arrivals depends on precise knowledge of the polarization of the shear-wave energy radiated into the anisotropic medium, and this can rarely be determined accurately enough from earthquake sources. Thus in analysing split shear-wave observations from local earthquakes as recorded on the TDP3 network, we are restricted to measurements of the first shear-wave polarization direction, and of the time delay between the split shear-waves.

4 The polarization of the first split shear-wave

Measurements of the horizontal polarization direction of the leading shear-wave arrivals were made for all earthquakes within the shear-wave window of each three-component station occupied during the TDP projects. The restriction imposed by the shear-wave window is important, since the waveform of the incident shear-wave is severely distorted outside the window by interaction with the free-surface. For plane waves in an isotropic halfspace, the aperture of the shear-wave window is defined by incidence angles less than the critical angle $\sin^{-1}(V_s/V_p)$, which is about 35^o for a Poisson's ration of 0.25 (Nuttli 1961, Evans 1984). In practice, the aperture is distorted by wavefront curvature, topography near the receiver, and possibly by the presence of low-velocity surface layers (Booth *et al.* 1985, Booth & Crampin 1985). Observed shear-wave arrivals may be assumed to be within the window so long as the shear-wave polarizations at the edge of the window are consistent with the pattern of polarizations well within the window. Particular caution is required when polarizations near the edge of the window are also consistent with the distorting effects of the free surface. We follow Booth *et al.* (1985) in setting the effective shear-wave window for the TDP stations at 40^o incidence angle.

The first shear-wave arrival could be clearly identified on 95% of the seismograms recorded within the shear-wave window. The polarization angle of the first shear-wave arrival in the horizontal plane was determined on polarization diagrams which had been rotated relative to the radial direction from source to receiver (examples are shown in the Appendix). The required geographical orientation of the first-arrival polarization-vector was obtained by adding the polarization angle relative to the radial direction to the azimuth of the station from the earthquake. This procedure helps to lessen any subjective bias in the measurements, by eliminating any tendency to settle for a specific geographical direction. In addition, the polarization measurements for the TDP1, TDP2 data and

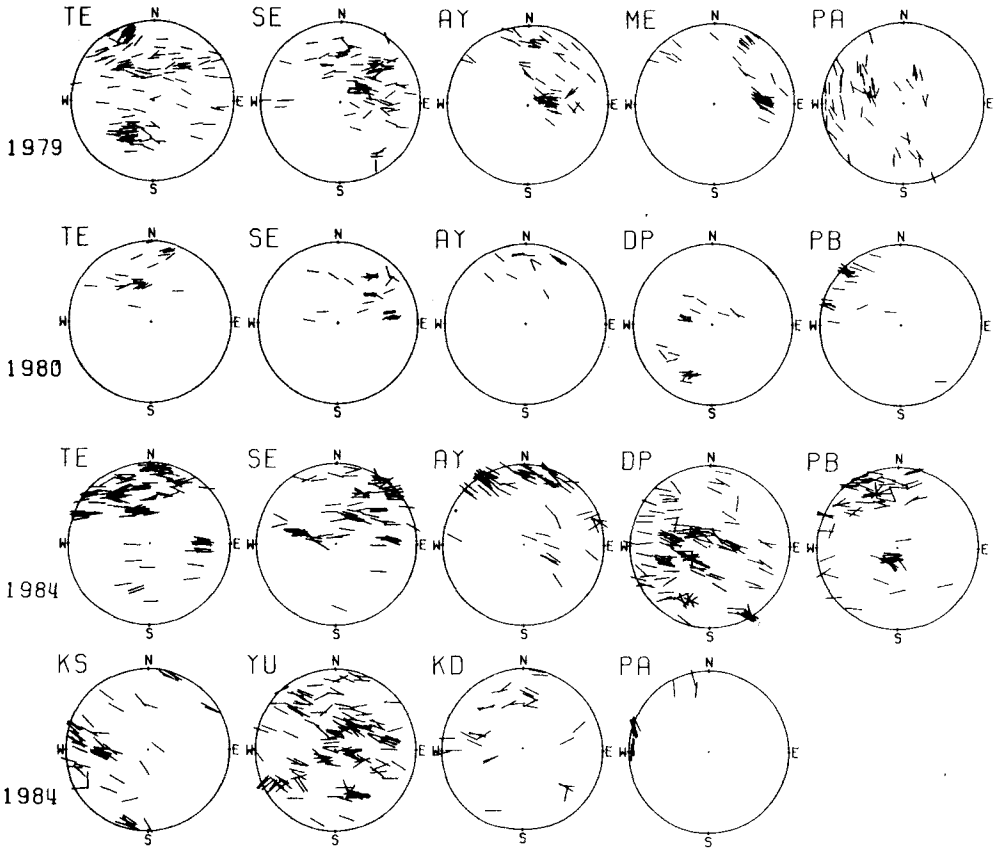

Figure 2. Horizontal projections of the polarizations of the leading shear-wave arrivals observed at TDP stations in 1979, 1980, and 1984, shown in equal-area projections of the lower hemisphere of directions out to incidence angles of 40^{o} beneath each station.

the TDP3 data were made independently (DCB and TC). Some seismograms recorded from events near the periphery of the shear-wave window (notably at station SE) exhibited the distinctive waveform characteristic of the local SP phase (Evans 1984, Booth & Crampin 1985). These seismograms were not used in this study.

4.1 OBSERVATIONS

The horizontal polarizations of the leading shear-wave arrivals from events at the TDP stations shown in Fig. 1 are shown in the equal-area projections in Fig. 2, and the angular distributions are shown as equal-area rose diagrams in the map in Fig. 3. We do not take account of the polarities of the polarizations in Figs. 2 and 3, as they are difficult to determine accurately. Note that we shall use *polarized* and *polarization* to refer to non-vector orientations (such as NE to SW), and *polarity* to

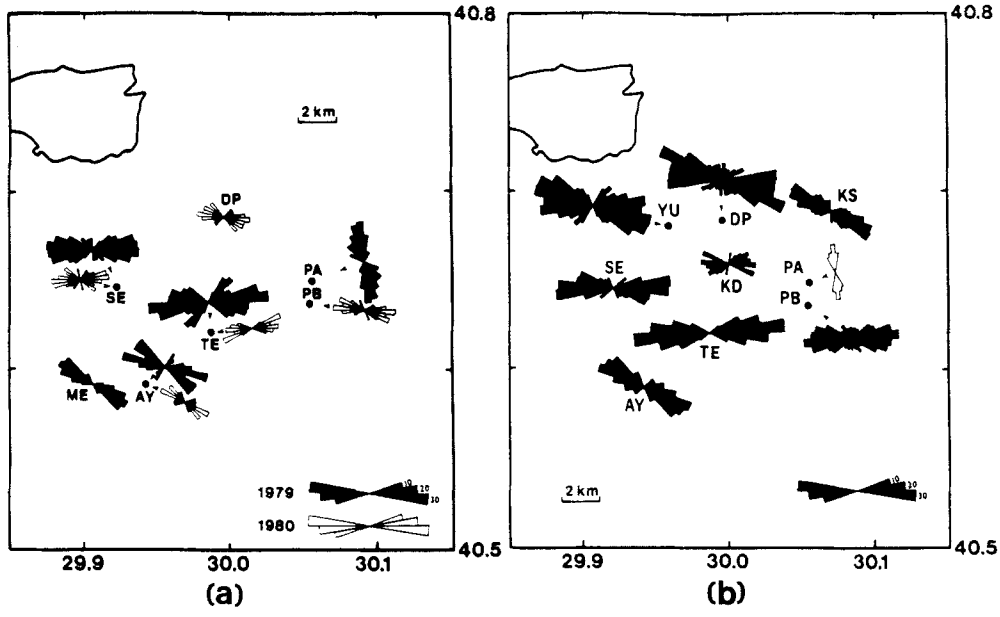

Figure 3. Equal-area rose diagrams of the distribution of polarization directions of the leading shear-wave observed at TDP stations (a) in 1979 and 1980, and (b) in 1984, for comparison. The polarizations observed at PA are believed to be spurious (see text) and are represented in Fig. 3(b) by an open rose.

refer to vector polarizations (such as NE or SW). The polarizations in Fig. 2 clearly display preferred directions of alignment, and the mean polarization direction at each station is, with one exception, within $\pm 20^{\circ}$ of N 100°E. The polarizations at the exceptional station, PA (Fig. 3), are discussed below. The distribution of epicentres within the shear-wave window at each station changes slightly in different years, but the preferred direction of polarization remains essentially the same.

4.2 INTERPRETATION

We follow Booth *et al.* (1985) and Crampin & Booth (1985) in showing that the polarization alignments observed at the TDP3 stations cannot be attributed to local effects at either source or receiver, but are consistent with the presence of effective anisotropy due to vertical EDA-cracks along much of the raypath.

Effect of topography

The topography of the region is steep and varied (Fig. 1), and the effect of scattering by the irregular topography must be expected. However, we follow Booth *et al.* (1985) in arguing that the evident consistency of

alignment of the polarizations at individual stations (from a wide variety of azimuths) and over all stations (with the exception of PA), suggests that topographic irregularities have only a secondary effect on the recorded polarizations of the first shear-wave arrival. Nevertheless, the topographic irregularities probably cause much of the scatter which is apparent in the polarization distributions in Figs. 2 and 3.

Polarization alignments produced by focal mechanisms

An earthquake source in an isotropic medium radiates shear waves which have polarizations and polarities which vary with direction and are fixed by the type and orientation of the focal mechanism. These alignments will be preserved at a receiver within the shear-wave window at the free surface, for the direct shear-wave arrival propagating through a homogeneous isotropic structure.

Lovell *et al.* (1987) have determined double-couple focal mechanisms from P-wave first motions for 32 earthquakes which occurred during the TDP3 experiment. Although several localized groups of events appear to have similar fault-plane solutions, there is a great variety of orientations in the set of solutions, subject only to consistent principal axes of stress. We have computed the shear-wave polarizations which would be generated on the surface of an isotropic halfspace by nine of the best-constrained fault-plane solutions of the larger events, and the polarizations are displayed in Fig. 4 as equal-area projections within the shear-wave window. It can be seen that the shear-wave polarizations radiated by these sources can be oriented in many different directions, and in particular there is not a dominant approximately east-west orientation.

The orientations of the observed shear-wave polarizations for these events are plotted for comparison on the projections at the appropriate location within the shear-wave window. Polarities have been assigned to the observed polarizations where the polarity of the first shear-wave arrival appears to be clear. The deviation between the observed and theoretical polarizations should be small if the material along the raypaths is isotropic. An inspection of Fig. 4 shows that, with one exception, this deviation is large unless the theoretical polarization is predominantly east-west oriented. The exception is the approximately north-south polarization recorded at station DP from focal mechanism 1, and this is discussed in the next section. The deviations between the observed and theoretical shear-wave polarizations indicate that the recorded polarization alignments cannot be due to earthquake focal mechanisms in an isotropic structure.

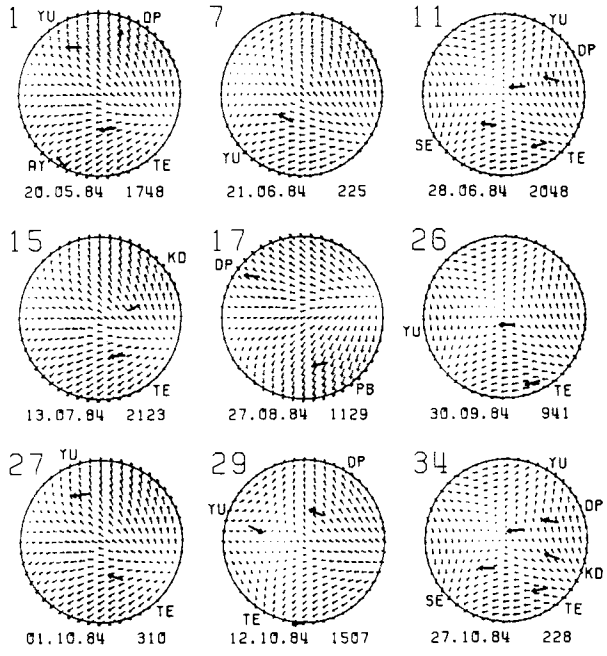

Figure 4. Equal-area projections, out to incidence angles of 40°, of the theoretical shear-wave polarizations generated by fault plane mechanisms for nine local earthquakes recorded by the TDP3 stations. The fault plane solutions are from Fig.3 of Lovell *et al.* (1987) and are numbered accordingly. The observed polarizations of the first-arriving shear-waves from these earthquakes at the named stations are shown as superimposed arrows.

Crack-induced anisotropy

Crampin & Booth (1985) have shown that the parallel polarizations of the first split shear-waves can be consistently interpreted in terms of propagation through a distribution of vertical liquid-filled cracks aligned approximately N 100°E. This orientation is consistent with cracks opening normal to the approximately north-south axis of minimum compression, which has been identified from fault-plane solutions (Crampin & Booth 1985; Crampin & Evans 1986; Lovell *et al.* 1987). Shear waves which propagate through such a system of approximately east-west oriented vertical cracks will split and, at angles of incidence within the shear-wave window, the first-arriving (faster) split shear-wave will be polarized in the N 100°E plane of the cracks (Crampin & Booth 1985). The second (slower) split shear-wave will be polarized approximately orthogonal to the faster shear-wave and to the direction of propagation, which corresponds closely to the north-south direction within the shear-wave window.

The relative amplitude and polarity of each split shear-wave will be determined by the orientation and polarity of the shear-wave polarization radiated in that direction by the source. Thus, most of the observed shear-wave polarizations in Fig. 4 show the approximately east-west polarization of the faster split shear-wave, parallel to the EDA-cracks. Their polarities correspond to the polarities of the east-west component of the shear-wave at the source. The only exception is the arrival at station DP in earthquake 1. In this case, the shear-wave polarization at the source is approximately north-south, and little or no energy propagates with the approximately east-west polarization of the faster shear-wave; only the slower split shear-wave propagates, with approximately north-south polarization.

Shear-wave splitting and polarization alignments have been observed in the records of earthquakes at depths ranging from less than 5 km to over 14 km. There is no correlation between the delay between the split shear-waves and the depth of focus, which implies that the distributions of EDA-cracks are present throughout most of the top 15 km of the crust in this area of Turkey. If the observed shear-wave splitting is caused by stress-aligned cracks, then a crucial observation would be a change in the characteristics of the shear-wave splitting with time. We would expect such a temporal variation to be correlated with changes in the ambient stress-field during an earthquake sequence (Crampin *et al.* 1984).

4.4 TEMPORAL VARIATION IN POLARIZATION

Polarization directions at PA

Booth *et al.* (1985) and Crampin & Booth (1985) noted that the directions of shear-wave polarization observed at station PA in 1979 were over 60^{o} different from the average alignment observed at all other stations in 1979 and 1980, including station PB, only 1.2 km away. Station PA was not used in 1980, since the site was very exposed on a steep hillside, and a more secure site was available at station PB. The difference in polarization directions observed between PA in 1979 and PB in 1980 led to the suggestion in Booth *et al.* (1985) and Crampin and Booth (1985) that there was "weak evidence" of a temporal variation of split shear-wave characteristics between 1979 and 1980 in the locality of PA and PB. It was speculated that the variation might be attributed to the release of a local stress anomaly by a very near earthquake occurring between 1979 and 1980. In order to test this hypothesis, station PA was re-occupied for a short time in 1984. In this section we re-examine the evidence for this temporal variation of leading shear-wave polarizations observed by the TDP

network.

Station PA was occupied only for a few weeks in 1984 before it was vandalized beyond recovery. (This was the only instance of serious damage in over 60 station years of BGS recording in Turkey.) However, nine earthquakes occurring within the shear-wave window were recorded, and the polarizations of the leading shear-wave are shown in Figs.2 and 3(a). The polarizations are oriented in the same direction as they were in 1979, and the difference in polarization direction between PA and the other stations of the TDP network cannot be attributed to a local change in the stress field.

A detailed examination of the three-component particle-motion of the three events recorded approximately N 20°W of PA in 1984 showed that the dominantly radial polarization of the first shear-wave arrival in the horizontal plane was not wholly shear-wave motion and was contaminated by P-wave motion. This suggests that the first supposedly shear-wave arrivals at PA suffer from interference with S-to-P conversions, which is not present at the nearby station PB or at the other stations. The polarizations of shear-wave first arrivals recorded at PA in 1979 were re-examined, and many polarizations in the sagittal plane showed the presence of S-to-P conversions.

The transverse polarizations observed near the western boundary of the shear-wave window in 1979 and 1984 (Fig. 2) show clear shear-wave polarization, oriented approximately north-south. However these transverse polarizations are probably the result of incidence at the free surface outside the shear-wave window. The station PA is located on a steep westward-facing slope of the highest mountain in the area. This situation has the effect of increasing the effective angle of incidence at the free surface for rays propagating upward from the west, so that the aperture of the effective shear-wave window is reduced in that direction. Most of the observations of shear-wave polarization for PA were assigned lower weights than the other stations, because the shear-wave was consistently more difficult to identify. Thus the difference in shear-wave polarization orientation between PA and PB is due to misinterpretation of the observations at PA, rather than a temporal variation of polarization direction.

Polarization directions at other TDP stations

A comparison of the polarization distributions observed at each station in different years (Fig. 3) shows that there is no evidence of a temporal variation of polarization directions. The average polarization direction measured at each TDP3 station in 1984 also showed no significant variation over a period of up to six months. Under the EDA hypothesis (Crampin et

al. 1984), the polarization direction of the first shear-wave within the shear-wave window is directly related to the orientation of the crack distribution, which is itself determined by the directions of the principal stresses in the dilatant region. The orientations of the principal axes of stress may not change significantly before an earthquake. It is more plausible that the magnitude of the stress will change, causing changes in crack dimensions and crack density. Such changes are expected to alter the magnitude and distribution of time delays between the split shear-waves. In the following section, we examine the time delay measurements made from the TDP experiments in 1979, 1980, and 1984, and analyse them for evidence of temporal variation.

In a complicated crustal structure influenced by the same regional stress-field it is likely that the alignment of EDA-cracks is likely to be similar even though the density and dimensions of the cracks may be different. That means that each material along the raypath is likely to have the same or similar anisotropic symmetry. Since numerical experiments show that the polarization of the leading (faster) split shear-wave is controlled by the symmetry along the raypath rather than the degree of velocity anisotropy, the general similarity of the symmetry means that the polarization of the leading split shear-wave is a comparatively stable parameter which is unlikely to be seriously disturbed. This is believed to be the reason for the remarkable near parallelism of polarizations at recording sites above small earthquakes in many very complicated geological structures around the world.

5 The time delay between the split shear-waves

The delay between the split shear-waves is a much more difficult parameter to identify than the first-arrival polarization. Each rock-type along a given raypath will have different crack densities, crack dimensions, and matrix velocities. While the symmetry of the crack geometry is likely to be approximately similar along the raypath, small changes at internal interfaces will cause further splitting of each split shear-wave passing through it. Thus although the polarization of the leading shear-wave is likely to be consistent, it will be followed, and the principal secondary split shear-wave is likely to be preceded, by a variety of further split shear-waves with different velocities and polarizations. The relative amplitudes and delays between these split shear-waves will vary with direction and make it very difficult to recognize any consistent second arrival in order to measure a time delay.

Shear-wave splitting is recognised in a polarization diagram by an abrupt change in polarization or ellipticity in the particle motion of the

leading shear-wave. Within the shear-wave window there is typically little P-wave coda and the shear-wave has an impulsive onset. Thus, the onset of the leading shear-wave can usually be picked reliably. However, identification of the onset of the second split shear-wave is often difficult for the reasons given above.

A procedure for the consistent measurement of time delay from the seismograms and polarization digrams is described in the Appendix. Although this procedure has been designed to be as objective as possible, there is still a degree of subjectivity associated with the identification of the exact onset of the two split shear-waves. To try to reduce this element of subjectivity, and to quantify to some extent the errors involved in delay measurement, measurements of delay were made by two independent observers (TC and DCB).

The time delay between split shear-waves depends on the length of the propagation path in the anisotropic medium, as well as the direction of the propagation path with respect to the anisotropic symmetry. Therefore we normalize the observed delay to the equivalent delay over a fixed path length of 1 km. In the absence of detailed knowledge of the velocity structure between source and receiver, we use a straight line propagation path to normalize the delays. Since the estimated path length depends on the earthquake location, we reject seismic records corresponding to locations with a low quality factor or root-mean-square residual of greater than 0.07, as computed by the HYP071 location program (Lee & Lahr 1975). Where doublet events (events with near-identical particle motion on all seismograms) occur within an interval of 24 hours, only the delay value corresponding to the first of the doublet sequence is included, to avoid biasing the distribution.

The two principal causes of a variation of time delays in a crack distribution would be a change in crack density, which could be caused either by increasing the number of cracks (by new cracks opening) or by increasing the dimensions of existing cracks (by crack growth), and/or a change in crack aspect-ratio (by existing cracks 'bowing'). Time delays in crack distributions possess a directional dependence according to the orientation of the propagation path with respect to the alignment of the crack planes, resulting in characteristic patterns of amplitude variation which are aligned by the crack geometry (Fig. 5). Crampin (1987a) has shown that changes in crack density and changes in crack aspect-ratio have different effects on these time-delay patterns, and these are illustrated in Fig. 5. Fig. 5(a) shows the contoured time delays for a distribution of parallel, vertical fluid-filled cracks aligned in an East-West direction, in an equal-area projection. An increase in the crack density of the

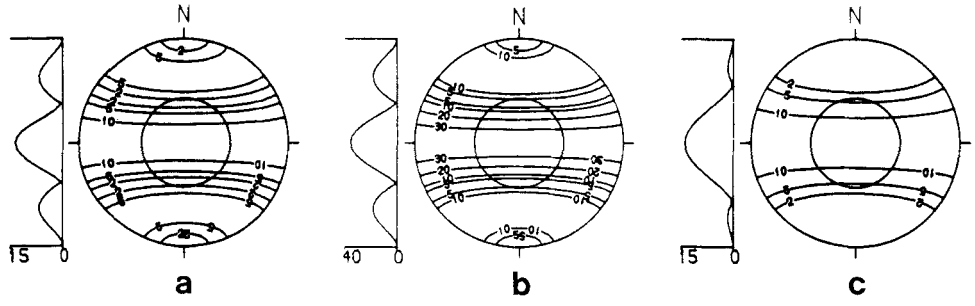

Figure 5. Equal-area projections out to 90° of the delays between split shear-waves propagating through an upper hemisphere of parallel, vertical water-filled cracks aligned in an East-West direction with (a) crack density CD = Na^3/v = 0.04 and aspect ratio AR = d/a = 0.001 (where N is the number of cracks of radius a in volume v and half-thickness d); (b) CD = 0.1 and AR = 0.001; and (c) CD=0.04 and AR=0.05. The delays are contoured in msec for path lengths of 1 km, and the circle within each projection indicates the approximate boundary of the shear-wave window. On the left of the projections is a North-South section of the delay contours. (After Crampin 1987a with elastic constants from Hudson 1980, 1981)

distribution (Fig. 5b) results in an increase in time delay between split shear-waves with propagation paths incident between 50° and 90° to the normals to the crack planes (Crampin 1987a). The time delays in Fig. 5(b) increase in a broad band aligned parallel to the strike of the cracks through the centre of the projection and throughout the shear-wave window. An increase in crack aspect-ratio, however, only increases the delays corresponding to propagation paths incident between about 50° and 75° to the crack normals (Fig. 5c). The delays in an East-West band across the centre of the projection, corresponding to propagation paths between 75° and 90° to the crack normals, are almost unchanged. Thus it is important to examine the observations of time delay in relation to their propagation path with respect to the crack geometry. In analysing time delays between split shear-waves recorded on the Anza network, Peacock *et al.* (1987) found that the temporal variation of the delays varied according to the direction of propagation with respect to the EDA crack-orientation as deduced from the polarization alignments.

Any perceived change of time delay with time may be due to the effect of a change in the raypath, rather than a temporal change in characteristics of the rockmass through which the waves propagate. The only way to ensure that the variation is due to the rockmass rather than the raypath is to repeat observations over the same raypath. In the present study with earthquake sources we have tried to minimize the effect of changes in

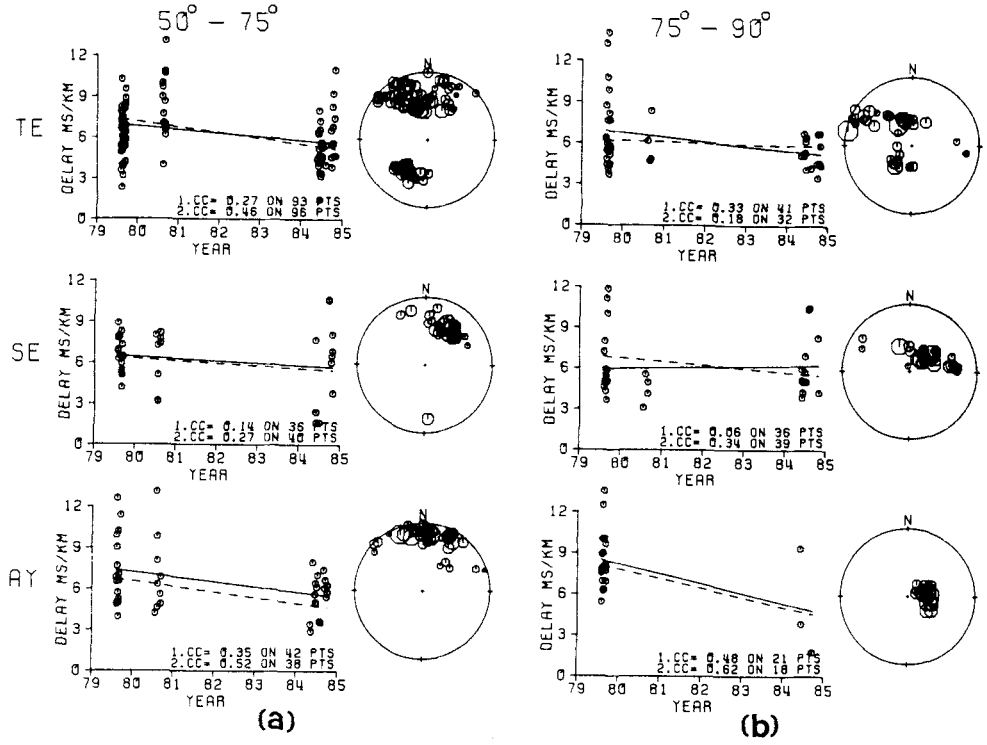

Figure 6. Variation of time delays between the split shear-waves in 1979, 1980, and 1984 from observations along raypaths which are incident between (a) 50° and 75°, and (b) 75° and 90° to the normal to a vertical plane aligned N 100°E. The solid line in the time distribution is the line of regression drawn through the observations made by observer 1, and the broken line is the regression line drawn through the equivalent observations (not shown) made by observer 2. The correlation coefficients (CC) of each regression line are given. The spatial distribution is plotted as an equal-area projection of the lower hemisphere beneath each station out to 40° incidence, and the area of each symbol is proportional to the delay.

raypath as far as possible, by eliminating single observations of time delays corresponding to directions which are widely different from others.

5.1 OBSERVATIONS

We have examined the observations of normalized time-delays in relation to the direction of their raypaths relative to the EDA crack orientation of N 100°E which has been deduced from the polarization alignments (Crampin & Booth 1985, and this study). We follow Peacock *et al.* (1987) and separate the time delays corresponding to raypaths incident between 50° and 75° to the crack normals from those corresponding to rays between 75° and 90° to the crack normals. The variation with time of delays measured at the three stations TE, SE, and AY (which were occupied in 1979, 1980, and 1984) are shown for the two ranges of incidence angle in Fig. 6, together

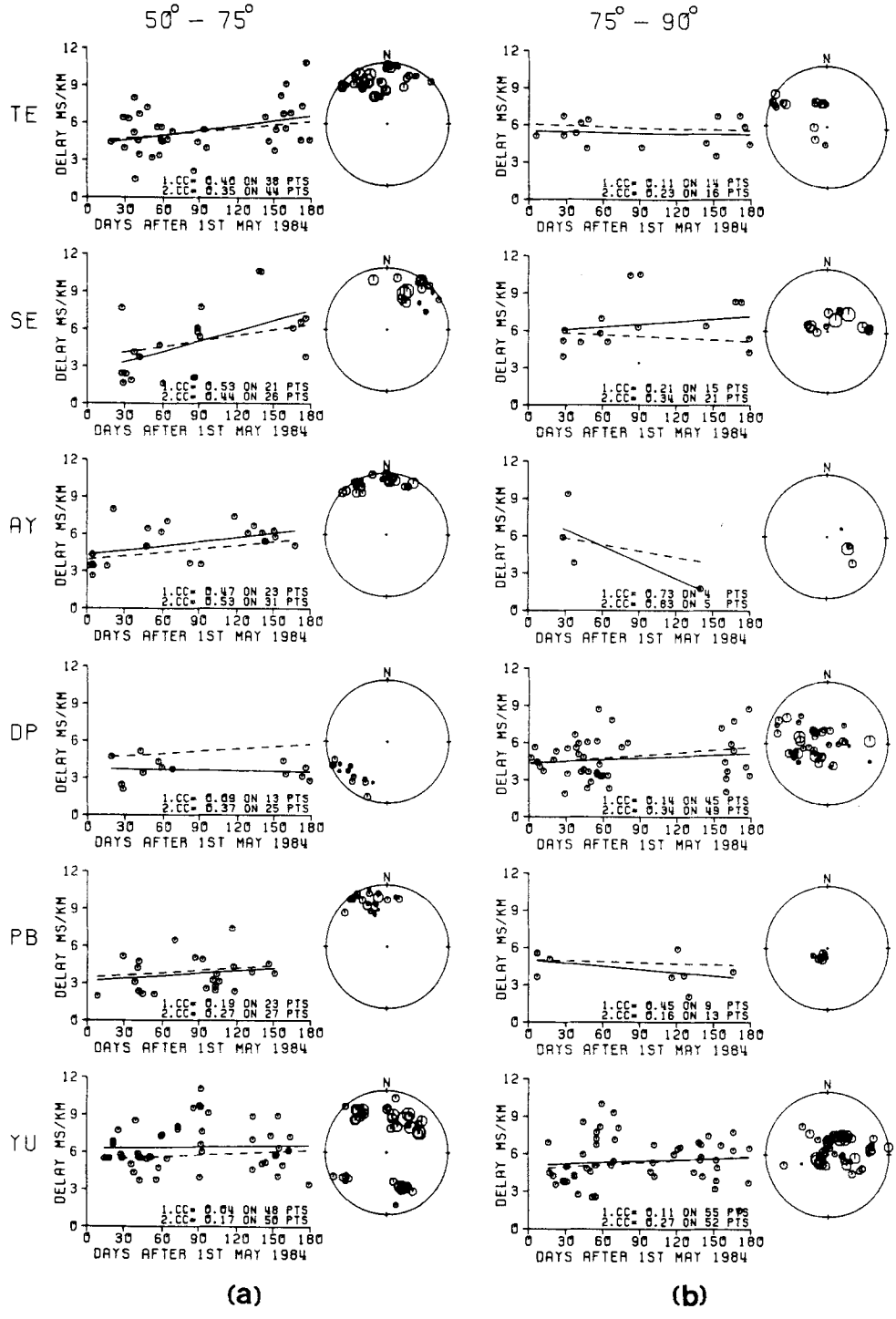

Figure 7. Shear-wave time delays in 1984, from observations along raypaths which are incident between (a) 50° and 75°, and (b) 75° and 90° to the normal to a vertical plane aligned N 100°E. Notation and symbols as in Fig. 6.

with their spatial distribution within the shear-wave window. Individual observations are shown only for observer 1. The solid line is the regression line of the data of observer 1, and the broken line is the regression line of the data of observer 2. The lines of regression do not have a well-defined meaning when applied to such an irregular distribution of data, and are included in Fig. 6 only to show the trend of the time variation. The variation of time delays at the six TDP3 stations recording over six months in 1984 is shown in Fig. 7, where again the delays have been separated into the same two ranges of incidence angle.

The distributions of observations at stations TE and DP in 1984 (Fig. 7) show two distinct bands. This was the result of the disruption of routine network maintenance necessitated by the temporary illness of the project leader. Note that shear-wave studies require each component of three-component instruments to be simultaneously operational and are consequently rather more sensitive to instrument malfunction than studies using conventional single-component networks.

5.2 INTERPRETATION

The delay between split shear-waves is dependent on the direction of propagation with respect to the crack orientation, and on the path length through the anisotropic medium. A migration of earthquake foci, or a systematically changing error in earthquake location, could cause an apparent temporal variation of the delays. Plots of variations of the hypocentres in time and space showed no significant variation which would lead to an apparent temporal change of delay, and they are not shown here.

The theoretical projections of delays in Fig. 5 suggest that maximum delay values should be concentrated in a band oriented N 100^{o}E through the centre of the shear-wave window. The distributions of delay magnitude in the equal-area projections of Figs. 6 and 7 show no apparent spatial pattern at any of the recording sites. However it is known that the delay between split shear-waves is much more sensitive to variations in the rock structure along the ray path than are the polarization directions (Peacock *et al.* 1987), and the lack of a spatial pattern is not unexpected.

Both observers find there is a small decrease in delay between 1979 and 1984 (Fig. 6) which is approximately the same for both ranges of incidence angle at stations TE and SE. At station AY insufficient data was recorded in the incidence range $75\text{-}90^{o}$ during 1984 for any comparison to be valid. The decrease over both ranges of incidence angle suggests that the temporal variation between 1979 and 1984 is more likely to be due to a decrease in crack density of the EDA-cracks than a decrease only in crack aspect-ratio.

Figure 7 shows the variation of time delays over six months in 1984. Three stations, TE, SE, and AY, show an increase in delay with time for paths between 50^{o} and 75^{o} to the crack normals which is significant at the 95% level. There is no significant temporal variation of delay at any station for paths in the $75\text{-}90^{o}$ range. At station DP there is insufficient data in the $50\text{-}70^{o}$ degree range for an assessment of temporal variation to be made, while at stations PB and YU the scatter in the data results in no significant temporal variation being apparent. According to the arguments given at the beginning of this section, the small but significant increase in delay with time observed at stations TE, SE, and AY for paths in the $50\text{-}75^{o}$ incidence range, but not for paths in the $75\text{-}90^{o}$ range, is suggestive of an increase in aspect ratio of the cracks in the hypothesized crack distribution. Such an increase could be caused by cracks 'bowing' due to an increase in the applied stress parallel to the crack faces or an increase in tension normal to the crack faces.

While the increase in delay with time at TE, SE, and AY in 1984 is statistically significant, the increase, of the order of 3 msec for a path length of 12 km over a period of 5 months, is small. Confirmation of a temporal variation requires the comparison of records of two events at the same location, separated in time. Lovell *et al.* (1987) have identified clusters of events at approximately the same locations, separated by up to three months and more, and these have been examined for supporting evidence of a temporal variation. The records for station AY in Fig. 8 show near-identical particle motions, with near-identical delays, over a period of three months. This observation effectively eliminates the possibility of a temporal variation observed over paths to AY in the six-month span of the 1984 project. However, a similar comparison of seismograms of events recorded at stations TE, SE, and AY from events at similar locations in 1979, 1980, and 1984 revealed no seismograms which were identical in different years. It follows that the temporal change shown in Fig. 6 for the five-year period 1979 to 1984 cannot be ruled out.

The delay distributions in Fig. 6 can be interpreted as indicating that there has been a small decrease in the crack density of the EDA crack distribution in the area of TDP stations TE, SE, and AY between 1979 and 1984. This would be consistent with a relaxation of the local stress-field between 1979 and 1984. It is not possible to determine from the available data whether the suggested change in stress field at the TDP stations from 1979 to 1984 reflects a local relaxation of stress after a local earthquake, or series of earthquakes, or whether it is due to a regional relaxation of stress after a larger earthquake farther away.

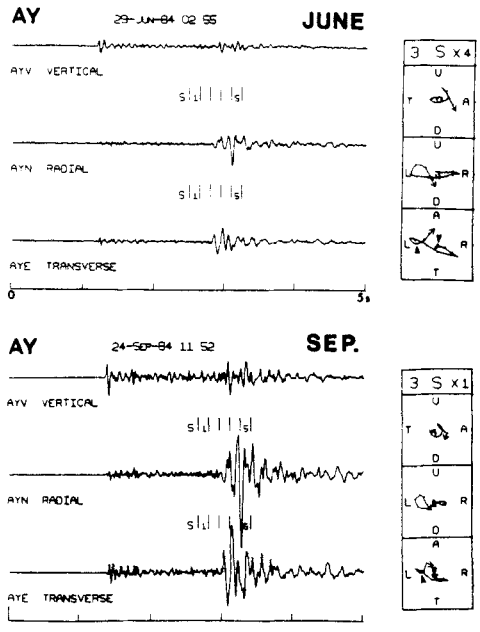

Figure 8. Seismograms of two earthquakes recorded by station AY, showing near-identical polarization diagrams and split shear-wave time delays over a period of three months. The numbered polarization diagram corresponds to the time interval 3 marked above the *S*-wave portion of the seismograms. It shows the shear-wave first arrivals in three mutually-orthogonal planes: from top to bottom, vertical-radial, vertical-transverse, and horizontal (labelled **Up**, **Down**, **Towards** and **Away** from the epicentre, and **Left** and **Right** of the radial direction away from the epicentre). Shear-wave splitting is seen in the horizontal plane; the onsets of the split shear-waves are indicated by arrows. Ticks on the particle displacements occur every 0.01s.

6 Conclusions

Shear-wave seismograms of local earthquakes recorded over six months near the North Anatolian Fault in the TDP3 experiment of 1984 have shown shear-wave splitting, with similar characteristics to that observed in the same area during TDP1 and TDP2 in 1979 and 1980. The shear-wave observations from all the TDP experiments are consistent with the presence of distributions of stress-aligned fluid-filled near-vertical cracks throughout the top 10-20 km of the crust. The significance of such extensive-dilatancy anisotropy is that is could be used to monitor stress changes in a seismic area, through the observation of temporal changes in the characteristics of the shear-wave splitting. In records from local earthquakes, the two measurable parameters which characterize the splitting are the polarization of the first split shear-wave and the time delay between

the split shear-waves. We have examined the data collected during TDP1, TDP2, and TDP3 for evidence of any temporal variation in these parameters.

There is no evidence for any significant change in the polarization direction of the first split shear-wave from 1979 to 1984, or over the six months of data available from TDP3. Under the EDA hypothesis, this indicates that there has been no change in the crack orientation, and hence no change in direction of the stress field which aligns the cracks, over these time intervals.

If the orientation of the stress-aligned cracks is constant, a temporal variation of the time delay between split shear-waves implies a change in crack dimensions or the crack density of the crack distribution. The distributions of delay times observed at the three stations which operated during all three TDP experiments indicate a possible small decrease in the crack density of the assumed crack distribution from 1979 to 1984 of approximately 0.001 per year. This observation suggests that the stress field in the TDP area decreased slightly between 1979 and 1984. A similar temporal variation in time delays was detected over a six-month period in 1984; however, seismograms of repeated events at the same location show no change in shear-wave delay times, throwing doubt on the 1984 observed trend. The polarization alignments over a wide area suggest that the extensive-dilatancy anisotropy is controlled by the regional stress-field, and so the absence of a short-term variation is perhaps not surprising.

The evidence presented above for a temporal variation of split shear-wave delays, implying a temporal variation in stress, cannot be regarded as conclusive. Confirmation of a temporal variation in time delays would require repeated observation of shear-wave arrivals over the same wave path. Thus the detection of a small temporal variation may not be possible using earthquake sources, which are too unreliable. Repeated shear-wave vertical-seismic profiles (VSPs) offer the best method for the detection of temporal variations in the characteristics of shear-wave splitting, although there is a limitation in that the depth at which temporal variations can be detected is determined by the depth of the well in which the instruments are located.

Acknowledgements

We thank Dr Ergun Toğrol, Rector of Boğaziçi University, and Dr Muammer Dizer, Balamir Üçer, and the rest of the staff at Kandilli Observatory for their support, without which this work would have been impossible. We gratefully acknowledge the work performed by the field staff, led by Russ Evans, throughout all the TDP experiments. The work was supported by the Overseas Development Administration, the Natural Environment Research

Council, and Boğaziçi University. The work of Tian-Chang Chen was supported by the Education Section of the Chinese Embassy. This work is published with the approval of the Director of the British Geological Survey (NERC), with some indirect support from US Geological Survey Grant 14-08-0001-G1380.

References

Atkinson, B.K., 1984. Subcritical crack growth in geologic materials, *J.geophys.Res*, **89**, 4077-4114.

Booth, D.C. & Crampin, S., 1985. Shear-wave polarizations on a curved wavefront at an isotropic free-surface, *Geophys.J.R.astr.Soc.*, **83**, 31-45.

Booth, D.C., Crampin, S., Evans, R. & Roberts, G., 1985. Shear-wave polarizations near the North Anatolian Fault - I. Evidence for anisotropy-induced shear-wave splitting, *Geophys.J.R.astr.Soc.*, **83**, 61-73.

Crampin, S., 1978. Seismic wave propagation through a cracked solid: polarization as a possible dilatancy diagnostic, *Geophys.J.R.astr.Soc.*, **53**, 467-496.

Crampin, S., 1981. A review of wave motion in anisotropic and cracked elastic-media, *Wave Motion*, **3**, 343-391.

Crampin, S., 1987a. The basis for earthquake prediction, *Geophys.J.R.astr.Soc.*, **91**, this issue.

Crampin, S., 1987b. The geological and industrial implications of extensive-dilatancy anisotropy, *Nature*, **328**, 491-496.

Crampin, S. & Atkinson, B.K., 1985. Microcracks in the Earth's crust, *First Break*, **3**, 16-20.

Crampin, S. & Booth, D.C., 1985. Shear-wave polarizations near the North Anatolian Fault - II. Interpretation in terms of crack-induced anisotropy, *Geophys.J.R.astr.Soc.*, **83**, 75-92.

Crampin, S., Bush, I., Naville, C. & Taylor, D.B., 1986. Estimating the internal structure of reservoirs with shear-wave VSPs, *The Leading Edge*, **5**, 35-39.

Crampin, S., Evans, R., Üçer, B., Doyle, M., Davis, J.P., Yegorkina, G.V. & Miller, A., 1980. Observations of dilatancy-induced polarization anomalies and earthquake prediction, *Nature*, **286**, 874-877.

Crampin, S., Evans, R. & Atkinson, B.K., 1984. Earthquake prediction: a new physical basis, *Geophys.J.R.astr.Soc.*, **76**, 147-156.

Crampin, S., Evans, R. & Üçer, S.B., 1985. Analysis of local earthquakes: the Turkish Dilatancy Projects (TDP1 and TDP2), *Geophys.J.R.astr.Soc.*, **83**, 1-16.

Crampin, S. & Evans, R., 1986. Neotectonics of the Marmara Sea region in Turkey, *J.geol.Soc.*, **143**, 343-348.

Evans, R., 1984. Effects of the free surface on shear wavetrains, *Geophys.J.R. astr.Soc.*, **76**, 165-172.

Hudson, J.A, 1980. Overall properties of a cracked solid, *Math.Proc.Camb.phil. Soc.*, **88**, 371-384.

Hudson, J.A., 1981. Wave speeds and attenuation of elastic waves in material containing cracks, *Geophys.J.R.astr.Soc.*, **64**, 133-150.

Kaneshima, S., Ando, M. & Crampin, S., 1987. Shear-wave splitting above small earthquakes in the Kinki district of Japan, *Phys.Earth Planet Int.*, **45**, 45-58.

Lee, W.H.L. & Lahr, J.C., 1975. HYPO71(revised): a computer program for determining hypocenter, magnitude, and fault motion patterns of local earthquakes, *Open File Rep. U.S.geol.Surv.*, 73-311.

Lovell, J., Crampin, S., Evans, R. & Üçer, S.B., 1987. Microearthquakes in the TDP swarm, Turkey: clustering in space and time, *Geophys.J.R.astr.Soc.*, **91**, this issue.

Nuttli, O., 1961. The effect of the Earth's surface on the *S*-wave particle motion, *Bull.seism.Soc.Am.*, **51**, 1429-1440.

Peacock, S., Crampin, S., Fletcher, J.B. & Booth, D.C., 1987. Shear-wave polarizations in the Anza seismic gap, Southern California: temporal changes as possible precursors, *J.geophys.Res.*, submitted.

Roberts, G., & Crampin, S., 1986. Shear-wave observations in a Hot-Dry-Rock geothermal reservoir: anisotropic effects of fractures, *Int.J. Rock Mech.Min.Sci.*, **23**, 291-302.

Appendix: The measurement of polarizations and time delays of split shear-waves

We suggest in Section 3 that only two parameters characterizing shear-wave splitting are quantifiable for earthquake sources. These are the polarization vector of the first split shear-wave, and the time delay between the split shear-waves. In this appendix we describe the procedures which were followed in order to measure polarizations and delays as objectively as possible.

DETERMINATION OF THE FIRST SHEAR-WAVE POLARIZATION VECTOR

The first step is to rotate the horizontal seismograms into components which are radial and transverse with respect to the line between epicentre and receiver. Since phase changes in the shear wavetrain associated with the splitting are often small and difficult to recognise on seismograms displayed as parallel time series, it is necessary to display the data in polarization diagrams. Polarization diagrams are three mutually perpendicular orthogonal sections of the particle displacements plotted for

successive time-intervals along the three-component wavetrains. The vertical sections are necessary only to distinguish between the shear-wave motion and possible *P*- or *S*-to-*P* converted waves. The horizontal section is the most important section for shear waves arriving in the shear-wave window at the surface above local earthquakes and it contains most of the shear-wave energy. Examples of rotated three-component seismograms of local events, and the corresponding polarization diagrams of the shear-wave motion, are shown in Fig.A1.

The most important step is the identification of the onset of the first shear-wave arrival; particular care should be taken over this. The vast majority of the TDP seismograms recorded in the shear-wave window showed clear impulsive onsets; seismograms showing emergent onsets were not used in this study. The particle motion of any shear-wave first arrivals with dominantly radial polarization in the horizontal plane was also examined in detail in order to reduce the chance of an *S*-to-*P* converted wave being misinterpreted as a shear-wave first arrival. The polarization direction of the first arrival in the horizontal plane is then determined from the corresponding polarization diagram. The first motion of the shear wave is usually sufficiently linear for the polarization direction to be identified. When interference of the *P*-wave coda and background noise results in slightly elliptical motion of the first shear-wave, the average polarization direction is chosen. Seismograms which show strongly elliptical or circular polarization of the first shear-wave are discarded. Where possible, vector polarizations are determined by assessing the sense (polarity) of the first motion. Measurements are weighted according to their perceived reliability.

DETERMINATION OF TIME DELAY

Measurement of the time delay requires identification of the onset of a second split shear-wave arrival. There are three types of difficulty: 1) for the reasons given in section 5 there may be a multiple choice of possible secondary split shear-waves so that no consistent suite of second arrivals can be identified even on records with good signal/noise ratios; and 2) second split shear-waves, like most second arrivals, may be obscured by both signal-generated coda and background noise. These may be particularly severe as the second split shear-wave arrivals follow so closely on the first arrival with delays of between (typically) zero and 0.15 seconds. (3) The shear waves radiated from the source may not excite both the possible polarizations equally, so that either split shear-wave may be very small or absent along any particular raypath. Nevertheless, despite these constraints, consistent arrivals can still be chosen in some circum-

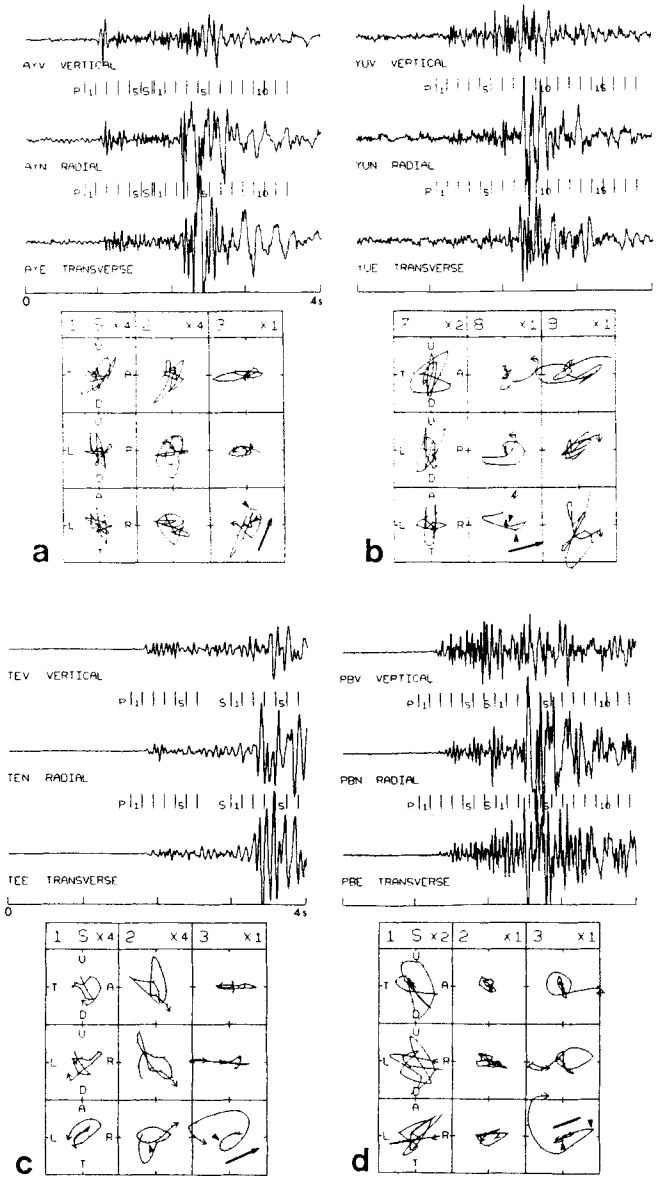

Figure A1. Typical seismograms of four different local earthquakes recorded by TDP3 stations. The recording stations, the focal depth and epicentral distance (in km), and the azimuth of the stations from the earthquakes are (a) AY, 7.1, 5.5, 96°; (b) YU, 7.5, 2.8, 196°; (c) TE, 10.5, 7.6, 204°; and (d) PB, 9.7, 1.0, 21°. Notation as in Fig. 8. The appropriate relative gain (e.g. ×2) is shown above each set of polarization diagrams and the solid bar indicates the vector polarization of the leading split shear-wave.

stances (Roberts & Crampin 1986; Kaneshima *et al.* 1986; Peacock *et al.* 1987).

Studies of synthetic seismograms (Crampin 1981) show that the onset of

second split shear-waves is marked by abrupt changes in the direction of the particle motion or ellipticity of the first shear-wave. Also, the change of any particular shear-wave arrival will vary with direction and may be small in any particular direction. The pronounced parallel alignment of the first shear-wave polarizations observed at TDP stations (Crampin & Booth 1985, and this study) strongly suggest that the observed shear-wave splitting is due to distributions of vertical, parallel saturated cracks. In this case, the polarization of the second split shear-wave is likely to be approximately (although seldom strictly) orthogonal to the polarization of the first shear wave throughout most of the shear-wave window (Crampin & Booth 1985). Therefore we define the onset of the second split shear-wave by a change of polarization of the first shear-wave, with a significant component of energy in the direction perpendicular to the first polarization direction. A 'significant component' is a component which is larger than the largest component of noise and/or *P*-wave coda in that direction in the previous two time windows. Rotation of the horizontal seismograms into components which are parallel and perpendicular to the direction of alignment of the first shear-wave polarization aids identification of the second split shear-wave onset. However it is normally identifiable on the polarization diagrams, from which the time delay can be measured from the number of data samples between the onsets of the first and second split shear-waves. The time delay measurement is also assigned a weight according to the relative reliability of the observation.

Examples of polarization vectors and split shear-wave onsets shown on the polarization diagrams in Fig.A1 were determined by the above procedures. Note that when there is a high signal-to-noise level, as at station PB in Fig.A1, the onset of the first shear-wave, and hence the polarity of first motion, cannot be precisely determined. This observation was assigned a relatively good weight for polarization direction, and a relatively poor weight for time delay.